Single Hole Green's Functions in Insulating Copper Oxides at Nonzero Temperature

J. van den Brink[a] and O. P. Sushkov[b]
School of Physics, The University of New South Wales, Sydney 2052, Australia

arXiv:cond-mat/9708159v1 21 Aug 1997

We consider the single hole dynamics in a modified $t-J$ model at finite temperature. The modified model includes a next nearest (t') and next-next nearest (t'') hopping. The model has been considered before in the zero temperature limit to explain angle resolved photo-emission measurements. We extend this consideration to the case of finite temperature where long-range anti-ferromagnetic order is destroyed, using the self-consistent Born approximation. The Dyson equation which relates the single hole Green's functions for a fixed pseudo-spin and for fixed spin is derived. The Green's function with fixed pseudo-spin is infrared stable but the Green's function with fixed spin is close to an infrared divergency. We demonstrate how to renormalize this Green's function in order to assure numerical convergence. At non-zero temperature the quasi-particle peaks are found to shift down in energy and to be broadened.

PACS numbers: 75.50.Ee, 75.10.Jm,

I. INTRODUCTION

Recent angle resolved photo-emission (ARPES) measurements by Wells *et al*[1] and by Pothuizen *et al*[2] on the insulating Copper Oxide $Sr_2CuO_2Cl_2$ provide an unique experimental probe of the properties of a single hole in an anti-ferromagnetic background. Theoretically this problem was analyzed in terms of a $t-t'-J$ model using exact diagonalization techniques for small clusters[3] and the self-consistent Born approximation (SCBA)[4]. From recent evaluation of the hopping integrals it was concluded that the next-next nearest neighbor hopping matrix element t'' is significant and almost as large as the diagonal hopping matrix element t', so that t'' should also be incorporated in a model Hamiltonian[5]. This was done in a recent paper[6], where also the leading corrections to the SCBA were evaluated.

The ARPES experiments[1,2] are carried out at a temperature of 300-350K, which is above the Neel temperature of this compound. Theoretical treatments up to now, however, restrict themselves to the zero temperature limit, assuming long range anti-ferromagnetic order, and spectra are artificially broadened in order to compare with experiment. It is therefore important to extend the SCBA calculations to finite temperature, where long range anti-ferromagnetic order is lacking, although at room temperature the magnetic correlation length for this compound is still about 60 lattice spacings and no drastic deviation of the ARPES spectrum at room temperature from the one at zero temperature is expected. Another motivation for this work is that a SCBA technique that can cope with the absence of long range magnetic order may be extended in the future to describe the spin liquid state of the doped copper oxides.

We consider a two-dimensional $t-t'-t''-J$ model at finite temperature. We apply the modified spin-wave theory suggested by Takahashi for 2D Heisenberg model at nonzero temperature[7] to deal with a state without long range anti-ferromagnetic order. The Hamiltonian for $t-t'-t''-J$ model is

$$H = -t\sum_{\langle ij\rangle\sigma} c^\dagger_{i\sigma}c_{j\sigma} - t'\sum_{\langle ij_1\rangle\sigma} c^\dagger_{i\sigma}c_{j_1\sigma} - t''\sum_{\langle ij_2\rangle\sigma} c^\dagger_{i\sigma}c_{j_2\sigma} + J\sum_{\langle ij\rangle\sigma}\mathbf{S}_i\mathbf{S}_j, \quad (1)$$

where $c^\dagger_{i\sigma}$ is the creation operator of an electron with spin σ ($\sigma=\uparrow,\downarrow$) at site i on the two-dimensional square lattice, $\langle ij\rangle$ represents nearest neighbor sites, $\langle ij_1\rangle$ next nearest neighbor sites (diagonal), and $\langle ij_2\rangle$ represents next-next nearest sites. The spin operator is $\mathbf{S}_i = \frac{1}{2}c^\dagger_{i\alpha}\sigma_{\alpha\beta}c_{i\beta}$. The exchange derived from two magnon Raman scattering is $J = 125meV$[8,9]. Following the most recent calculation of the hopping matrix elements performed by Andersen *et al*[5] we take: $t = 386meV$, $t' = -105meV$, $t'' = 86meV$. We set $J = 1$, so that in these units

$$t = 3.1, \quad t' = -0.8, \quad t'' = 0.7 \quad (2)$$

We first calculate the hole Green's function with fixed pseudo-spin at finite temperature, introduced by a constraint on the sub-lattice magnetization, and evaluate the contribution to the self energy due to the virtual absorption of spin-waves by the hole. Then the hole Green's function with fixed spin, that corresponds to Green's function that is actually measured in ARPES, is calculated. This Green's function turns out to be close an infrared divergency and we show that this instability can be avoided by a proper renormalization, assuring that the results numerically converge even when a rather limited number of grid-points is used. We find that at non-zero temperature the quasi-particle peaks broaden and shift to lower energy. The shift is independent of momentum and is due to the larger effective hole bandwidth as at finite temperature the spin order is frustrated.

II. HOLE GREEN'S FUNCTION WITH FIXED PSEUDO-SPIN G_D

At half filling (one electron per site) the model under consideration is equivalent to a Heisenberg model. We

are interested in the situation when one electron is removed from the system, when a single hole is produced. The dynamics of a single hole in an anti-ferromagnetic background can be described by SCBA[10,11]. This approximation works very well due to the absence of a single loop corrections to the hole-spin-wave vertex[12–14]. Now we have to modify SCBA for finite temperature. The main complication is that at finite temperature there is no long range anti-ferromagnetic order. Nevertheless, following Takahashi[7] we introduce artificially two sublattices: up and down. The bare hole operator d_i is defined so that $d_i^\dagger \propto c_{i\uparrow}$ on the $\uparrow$ sub-lattice and $\propto c_{i\downarrow}$ on the $\downarrow$ sub-lattice. In momentum representation

$$d^\dagger_{\mathbf{k}\downarrow} = \sqrt{\frac{2}{N(1/2+m)}} \sum_{i\in\uparrow} c_{i\uparrow} e^{i\mathbf{k}\mathbf{r}_i}$$
$$d^\dagger_{\mathbf{k}\uparrow} = \sqrt{\frac{2}{N(1/2+m)}} \sum_{j\in\downarrow} c_{j\downarrow} e^{i\mathbf{k}\mathbf{r}_j}, \qquad (3)$$

where N is number of sites and $m = \langle S_{iz}\rangle = 0$ is the average magnetization. The brackets $\langle\rangle$ denote both quantum and statistical averaging. The quasi-momentum $\mathbf{k}$ is restricted to be inside the magnetic Brillouin zone: $\gamma_{\mathbf{k}} = \frac{1}{2}(\cos k_x + \cos k_y) \geq 0$. In this notations it looks like $d_{\mathbf{k}\sigma}$ has spin $\sigma = \pm 1/2$, but actually rotation invariance is violated and σ is a pseudo-spin which just labels the two sub-lattices. Nevertheless the pseudo-spin gives the correct value of the spin z-projection: $S_z = \sigma = \pm 1/2$. The coefficients in (3) provide the correct normalization:

$$\langle d_{\mathbf{k}\downarrow} d^\dagger_{\mathbf{k}\downarrow}\rangle = \frac{4}{N}\sum_{i\in\uparrow}\langle c^\dagger_{i\uparrow} c_{i\uparrow}\rangle = 2\left(\frac{1}{2} + \langle S_{iz}\rangle\right) = 1. \qquad (4)$$

The retarded hole Green's function is defined as

$$G_d(\epsilon, \mathbf{k}) = -i\int_0^\infty \langle d_{\mathbf{k}\sigma}(\tau) d^\dagger_{\mathbf{k}\sigma}(0)\rangle e^{i\epsilon\tau} d\tau \qquad (5)$$

The t', t'' terms in the Hamiltonian (1) correspond to the hole hopping inside one sub-lattice. This gives the bare hole dispersion

$$\begin{aligned}\epsilon_{0\mathbf{k}} &= 4t'\cos k_x \cos k_y + 2t''(\cos 2k_x + \cos 2k_y) \\ &\to \beta_{01}\gamma^2_{\mathbf{k}} + \beta_{02}(\gamma^-_{\mathbf{k}})^2, \end{aligned} \qquad (6)$$

where $\gamma^-_{\mathbf{k}} = \frac{1}{2}(\cos k_x - \cos k_y)$, $\beta_{01} = 4(2t'' + t')$, and $\beta_{02} = 4(2t'' - t')$. In equation (6) we took into account that the sign of a hole dispersion is opposite to that for an electron (the maximum of the electron band corresponds to the minimum of the hole band), and omitted the constant term. The bare hole Green's function is

$$G_{0d}(\epsilon, \mathbf{k}) = \frac{1}{\epsilon - \epsilon_{0\mathbf{k}} + i0}. \qquad (7)$$

For spin excitations we use the modified spin-wave theory[7] (see also review paper[15]). In order to treat the Heisenberg term in the Hamiltonian (1) within spin-wave theory, it is convenient to use the Dyson-Maleev transformation[16] for a localized spin $S = 1/2$,

$$\begin{aligned} &S^-_l = a^\dagger_l, \quad S^+_l = (2S - a^\dagger_l a_l)a_l, \\ &S^z_l = S - a^\dagger_l a_l, \quad for \;\; l \in up \;\; sublattice; \\ &S^-_m = b_m, \quad S^+_m = b^\dagger_m(2S - b^\dagger_m b_m), \\ &S^z_m = -S + b^\dagger_m b_m, \quad for \;\; m \in down \;\; sublattice, \end{aligned} \qquad (8)$$

and the Fourier representation for a_l and b_m:

$$a_l = \sqrt{\frac{2}{N}}\sum_{\mathbf{q}} e^{i\mathbf{q}\mathbf{r}_l} a_{\mathbf{q}} \qquad (9)$$
$$a_m = \sqrt{\frac{2}{N}}\sum_{\mathbf{q}} e^{i\mathbf{q}\mathbf{r}_m} b_{\mathbf{q}}.$$

The summation over $\mathbf{q}$, here and everywhere below, is restricted inside the magnetic Brillouin zone. There are essentially two ways to find an effective Hamiltonian quadratic in the operators a and b. The first way is just to drop the quartic terms as is done in linear spin-wave theory (LSWT). The second way is to treat the quartic terms at mean-field level $a^\dagger a b^\dagger b \to \langle a^\dagger a\rangle b^\dagger b + \langle a^\dagger b^\dagger\rangle ab + ...$, corresponding to mean field spin-wave theory. As both approximations give very close results we choose use LSWT because it is simpler in the present context.

A. Finite Temperature Correction for G_d

So far we followed the zero temperature derivation for the SCBA. We take the approach of calculating the finite temperature corrections to the hole Green's function G_d with a diagrammatic, perturbative, method. This framework can be used if the number of spin-waves per site is small, i.e. if T/J is not too large. This is a reasonable pre-requisition as in the experiments T/J is of the order of $1/4$. We will show later on that at these temperatures the number of spin-waves is actually small, justifying our approach. The advantage of this approach over performing the calculations at imaginary, Matsubara, frequencies is that in our framework the absence of long-range antiferromagnetic order is specifically built in. Also problems with the numerical analytic continuation on the real frequency axis are avoided. As is shown later on, an almost-divergency occurs that demands large lattices in order to get stable results. By performing the calculation on the real axis from the beginning, the Green's function can be renormalized, lifting the almost-divergency.

At non-zero temperatures the long range antiferromagnetic order is destroyed. Very many long-wavelength spin waves are excited, and one must take into account their non-linear interaction. An approximate way to do it is to impose an additional condition that the sub-lattice magnetization is zero[7].

$$\langle S^z_{l\in\uparrow} - S^z_{m\in\downarrow}\rangle = \langle \frac{1}{2} - a^\dagger_{\mathbf{l}} a_{\mathbf{l}} + \frac{1}{2} - b^\dagger_{\mathbf{m}} b_{\mathbf{m}}\rangle = 0. \quad (10)$$

This constraint gives an effective cutoff of unphysical states in Dyson-Maleev transformation. The constraint (10) is introduced into the Hamiltonian via a Lagrange multiplier $\frac{1}{8}\nu^2$. Now we must diagonalize

$$\begin{aligned} H_{eff} &= H_{LSWT} - \frac{1}{8}\nu^2 (S^z_{l\in\uparrow} - S^z_{m\in\downarrow}) \quad (11)\\ &\to 2\sum_{\mathbf{q}} \left(A(a^\dagger_{\mathbf{q}} a_{\mathbf{q}} + b^\dagger_{\mathbf{q}} b_{\mathbf{q}}) + \gamma_{\mathbf{q}} (a_{\mathbf{q}} b_{-\mathbf{q}} + a^\dagger_{\mathbf{q}} b^\dagger_{-\mathbf{q}}) \right), \end{aligned}$$

where $A = 1 + \nu^2/8$. This can be done by the Bogoliubov transformation

$$\begin{aligned} a_{\mathbf{q}} &= u_{\mathbf{q}} \alpha_{\mathbf{q}} + v_{\mathbf{q}} \beta^\dagger_{-\mathbf{q}}, \quad (12)\\ b_{-\mathbf{q}} &= v_{\mathbf{q}} \alpha^\dagger_{\mathbf{q}} + u_{\mathbf{q}} \beta_{-\mathbf{q}}, \end{aligned}$$

and we find the effective spectrum and Bogoliubov parameters

$$\begin{aligned} \omega_{\nu\mathbf{q}} &= 2\sqrt{A^2 - \gamma^2_{\mathbf{q}}},\\ u_{\mathbf{q}} &= \sqrt{\frac{A}{\omega_{\nu\mathbf{q}}} + \frac{1}{2}}, \quad (13)\\ v_{\mathbf{q}} &= -sign(\gamma_{\mathbf{q}}) \sqrt{\frac{A}{\omega_{\nu\mathbf{q}}} - \frac{1}{2}}. \end{aligned}$$

These equation show that at non-zero temperature the spin-wave spectrum has a gap $\nu\sqrt{1 + \frac{\nu^2}{16}} \approx \nu$. This elucidates the meaning of the constraint and the Lagrange multiplier. Taking into account that in thermal equilibrium

$$n_{\mathbf{q}} \equiv \langle \alpha^\dagger_{\mathbf{q}} \alpha_{\mathbf{q}}\rangle = \langle \beta^\dagger_{\mathbf{q}} \beta_{\mathbf{q}}\rangle = \frac{1}{\exp(\omega_{\nu\mathbf{q}}/T) - 1} \quad (14)$$

we obtain from (10) the equation for ν

$$0 = 1 - \frac{2}{N}\sum_{\mathbf{q}} \frac{A}{\omega_{\nu\mathbf{q}}}(1 + 2n_{\mathbf{q}}). \quad (15)$$

This equation gives an exponentially small ν, and hence an exponentially large magnetic correlation length $\xi_M \propto 1/\nu$.

Hopping to a nearest neighbor in the Hamiltonian (1) gives an interaction of the hole with spin-waves.

$$\begin{aligned} H_{h,sw} = \sum_{\mathbf{k},\mathbf{q}} g_{\mathbf{k},\mathbf{q}} (&d^\dagger_{\mathbf{k}+\mathbf{q}\downarrow} d_{\mathbf{k}\uparrow} \alpha_{\mathbf{q}}\\ &+ d^\dagger_{\mathbf{k}+\mathbf{q}\uparrow} d_{\mathbf{k}\downarrow} \beta_{\mathbf{q}} + H.c.). \quad (16) \end{aligned}$$

In diagrams we will denote the vertex $g_{\mathbf{k},\mathbf{q}}$ by a dot, see figure 3d. This vertex is given by

$$\begin{aligned} g_{\mathbf{k},\mathbf{q}} &\equiv \langle \alpha_{\mathbf{q}} d_{\mathbf{k}\uparrow} | H_t | d^\dagger_{\mathbf{k}+\mathbf{q}\downarrow}\rangle\\ &= 4t\sqrt{\frac{2}{N}}(\gamma_{\mathbf{k}} u_{\mathbf{q}} + \gamma_{\mathbf{k}+\mathbf{q}} v_{\mathbf{q}}). \quad (17) \end{aligned}$$

In this calculation the usual mean field factorization approximation

$$\langle \alpha_{\mathbf{q}} c^\dagger_{j\downarrow} c_{j\uparrow} c^\dagger_{i\uparrow} c_{i\uparrow}\rangle \approx \langle \alpha_{\mathbf{q}} c^\dagger_{j\downarrow} c_{j\uparrow}\rangle \langle c^\dagger_{i\uparrow} c_{i\uparrow}\rangle = 1/2 \cdot \langle \alpha_{\mathbf{q}} S^-_j\rangle$$

has been used. For simplicity we have omitted in the calculation (17) the standard Bose statistics factor $\sqrt{1 + n_{\mathbf{q}}}$, but they are certainly taken into account in the calculation of diagrams. We stress that the vertex (17) has the same form as in the case of zero temperature, except for the pseudo-gap in the Bogoliubov parameters (13). We remind of the fact that at zero temperature $g_{\mathbf{k},\mathbf{q}=0} = 0$ because of the Goldstone theorem. In the present case due to the pseudo-gap $g_{\mathbf{k},\mathbf{q}=0} \neq 0$. This is a reflection of the fact that the long range anti-ferromagnetic order is destroyed. However, as the pseudo-gap is small, its presence will not give rise to large effects in the spectra.

FIG. 1. Self energy at finite temperature. The solid line represents the hole Green's function G_d, and the dashed line represents the spin-wave. The first diagram corresponds to virtual emission of the spin wave, and the second diagram corresponds to virtual absorption.

Similar to the zero temperature case the spin structure of the interaction (16) forbids single loop corrections to the hole-spin-wave vertex, so that the self energy is of the form

$$\begin{aligned} \Sigma(\epsilon, \mathbf{k}) = \sum_{\mathbf{q}} [&(1 + n_{\mathbf{q}}) g^2_{\mathbf{k}-\mathbf{q},\mathbf{q}} G_d(\epsilon - \omega_{\mathbf{q}}, \mathbf{k} - \mathbf{q})\\ &+ n_{\mathbf{q}} g^2_{\mathbf{k},\mathbf{q}} G_d(\epsilon + \omega_{\mathbf{q}}, \mathbf{k} + \mathbf{q})]), \quad (18) \end{aligned}$$

where first term arises from the virtual emission of the spin wave and second term arises from the virtual absorption, see figure 1. The self-consistent solution of this equation together with the standard relation

$$G_d(\epsilon, \mathbf{k}) = \frac{1}{\epsilon - \epsilon_{0\mathbf{k}} - \Sigma(\epsilon, \mathbf{k}) + i0}, \quad (19)$$

gives the retarded Green's function. Due to the definition of the operators (3) the Green's function (5) is invariant under translation with the inverse vector of the magnetic sub-lattice $\mathbf{Q} = (\pm\pi, \pm\pi)$

$$G_d(\epsilon, \mathbf{k} + \mathbf{Q}) = G_d(\epsilon, \mathbf{k}) \quad (20)$$

in spite of the absence of the long range anti-ferromagnetic order.

B. Results for $\mathbf{G}_d$

The numerical solution of equation (19) is straightforward. To avoid poles we replace $i0 \to i\Gamma/2 = i\ 0.05$. The energy scale consists of 300 points with variable density (concentrated near sharp structures of G_d). The number of points in the magnetic Brillouin zone is 10^4 which is equivalent to a 140×140 lattice. Actually the results are almost independent of the grid as soon as it is larger than 20×20. In figure 2 $-\frac{1}{\pi}\ Im\ G_d(\omega, \mathbf{k})$ as a function of ω for a cut through the Brillouin zone from $\mathbf{k} = (\pi/2, \pi/2)$ to $\mathbf{k} = (\pi, 0)$ is shown for two different temperatures.

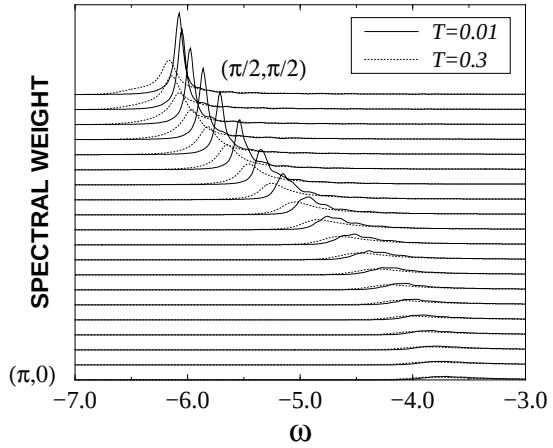

FIG. 2. Plots of $-\frac{1}{\pi}\ Im\ G_d(\omega, \mathbf{k})$ as a function of ω for a cut through the Brillouin zone from $\mathbf{k} = (\pi/2, \pi/2)$ to $\mathbf{k} = (\pi, 0)$ for T=0.01 and T=0.3.

The number of spin-waves per site for the highest temperature, $T = 0.4$, we considered, is ≈ 0.05, so much smaller than unity, justifying the perturbational approach. We recall that we use the set of parameters (2) based on Ref.[5]. The same set has been used in Ref.[6] for a zero temperature calculation. Quasiparticle energies and residues obtained here are quite similar to that at zero temperature[6]. We see from figure 2 that temperature shifts the quasi-peaks positions to lower energy and broadens them. The explanation for this is that there are two contributions to the self-energy at non-zero temperatures. One term originates from virtual spin-wave emission processes and the other from virtual spin-wave absorption. The former contribution is also present at T=0 and is enhanced at finite temperatures by a factor $1 + n_{\mathbf{q}}$, i.e. at finite temperature the interaction between the spin-waves and the hole is effectively increased due to this process. The matrix element for emission of an extra spin-wave is larger if the number of spin-waves already present is larger, because of the bosonic nature of the spin-waves. The part of the self-energy that is due to the spin-wave emission is multiplied by a factor larger than one at finite temperature, causing a shift of the quasiparticle peaks to lower energy that is nearly uniform in the Brillouin zone and a shift of the incoherent part of the Greens' function to higher energies. This has a simple physical reason. At non-zero temperature the hole propagates more easily because the anti-ferromagnetic order is frustrated. This causes a uniform shift of all quasiparticle poles to lower energy and does not effect their dispersion, as the quasiparticle dispersion is determined predominantly by the magnetic interaction. So the effect of non-zero temperature is qualitatively different from the effects of doping, where it is found that a reconstruction of the quasiparticle dispersion takes place, attributed to the frustrated magnetic order in the doped system[17]. The contribution to the self-energy at finite temperature because of the spin-wave absorption is mainly responsible for the broadening of the quasi-particle peaks.

III. HOLE GREEN'S FUNCTION WITH FIXED SPIN $\mathbf{G}_C$

The operators $d_{\mathbf{k}\uparrow}$, $d_{\mathbf{k}\downarrow}$ discussed in the previous section are defined at different sub-lattices. The operators on two sub-lattices are useful as mathematical constructions but when a photon removes an electron from the system, it does not differentiate between the sub-lattices, and moreover, at nonzero temperature there are no sub-lattices at all. Therefor we have to define the particle operator that is relevant for photo-emission independent of the sub-lattice. This particle operator is:

$$c_{\mathbf{k}\sigma} = \sqrt{\frac{2}{N}} \sum_i c_{i\sigma} e^{i\mathbf{k}\mathbf{r}_i}. \tag{21}$$

The normalization is chosen in such a way that

$$\langle 0 | c^\dagger_{\mathbf{k}\uparrow} c_{\mathbf{k}\uparrow} | 0 \rangle = \frac{2}{N} \langle 0 | \sum_i c^\dagger_{i\uparrow} c_{i\uparrow} | 0 \rangle = 1. \tag{22}$$

The corresponding retarded Green's function is

$$G_c(\epsilon, \mathbf{k}) = -i \int_0^\infty \langle c^\dagger_{\mathbf{k}\sigma}(\tau) c_{\mathbf{k}\sigma}(0) \rangle e^{i\epsilon\tau} d\tau. \tag{23}$$

This is the Green's function measured in ARPES.

Now we have to find the relation between $G_c(\epsilon, \mathbf{k})$ and $G_d(\epsilon, \mathbf{k})$. The operator $c_{\mathbf{k}\sigma}$ acting on half filled ground-state produces a single hole. We denote the corresponding amplitude by $a_{\mathbf{k}}$ and denote it in figure 3a as a cross. The thick line corresponds to the Green's function G_c (23) and the thin line corresponds to the G_d (5). The amplitude $a_{\mathbf{k}}$ equals

$$a_{\mathbf{k}} = \langle d_{\mathbf{k}\uparrow} c_{\mathbf{k}\downarrow} \rangle = \sqrt{\frac{1}{2}}. \tag{24}$$

The operator $c_{\mathbf{k}\sigma}$ acting on a state of the system can also produce a hole + spin-wave. This amplitude is shown in figure 3b as a circled cross with the dashed line being a spin-wave. We denote this amplitude by $b_{\mathbf{k},\mathbf{q}}$

$$b_{\mathbf{k-q},\mathbf{q}} = \langle \beta_{\mathbf{q}} d_{\mathbf{k-q}\downarrow} c_{\mathbf{k}\downarrow} \rangle$$
$$= \frac{2\sqrt{2}}{N} \langle \beta_{\mathbf{q}} \left(\sum_{i\in\uparrow} S_i^+ e^{i\mathbf{q}\mathbf{r_i}} \right) \rangle \qquad (25)$$
$$= \frac{2\sqrt{2}}{N} \langle \beta_{\mathbf{q}} \left(\sum_{i\in\uparrow} (1 - a_i^\dagger a_i) a_i e^{i\mathbf{q}\mathbf{r_i}} \right) \rangle \approx \sqrt{\frac{2}{N}} v_{\mathbf{q}}.$$

There is some ambiguity in the last step of this derivation. If we neglect the quartic term $\beta_{\mathbf{q}}(1-a_i^\dagger a_i)a_i \to \beta_{\mathbf{q}} a_i$ we get a value of $b_{\mathbf{k},\mathbf{q}}$ by a factor $\sqrt{2}$ larger than that given by eq. (25). If we treat the quartic term on a mean field level then $a_i^\dagger a_i \to 1/2$ and we get a value of $b_{\mathbf{k},\mathbf{q}}$, a factor $\sqrt{2}$ smaller than in eq.(25). The correct value is somewhere in between. We choose the vertex $b_{\mathbf{k},\mathbf{q}}$ to be the same as in the zero temperature case[6]. We will see that this provides the correct sum rule for the Green's function G_c, and this is a justification of our choice. We stress that (25) is a bare vertex. It corresponds to the instantaneous creation of a hole + spin-wave, but not the creation of a hole with a subsequent decay into a hole + spin-wave.

A. Finite Temperature Correction for $\mathbf{G}_c$

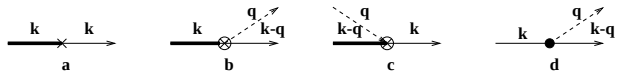

FIG. 3. The vertices: a) - single hole creation, b) - hole + spin-wave creation, c) - hole creation with spin wave annihilation, g) - usual hole-spin-wave vertex. The thick line correspond to G_c, and the thin solid line corresponds to G_d. The dashed line is the spin-wave.

At finite temperature there is another possibility: the creation of a hole with the absorption of a spin wave from the thermal bath. We denote this amplitude by $c_{\mathbf{k},\mathbf{q}}$. It is shown in figure 3c, and for simplicity we also denote it as a circled cross. The derivation of $c_{\mathbf{k},\mathbf{q}}$ is quite similar to (25) and the result is

$$c_{\mathbf{k},\mathbf{q}} = \langle \alpha_{-\mathbf{q}}^\dagger d_{\mathbf{k-q}\downarrow} c_{\mathbf{k}\downarrow} \rangle \approx \sqrt{\frac{2}{N}} u_{\mathbf{q}}. \qquad (26)$$

In eqs. (25) and (26) we have omitted the standard Bose statistics factors $\sqrt{1+n_{\mathbf{q}}}$ in (25) and $\sqrt{n_{\mathbf{q}}}$ in (26). These factors are taken into account separately in the calculation of the diagrams.

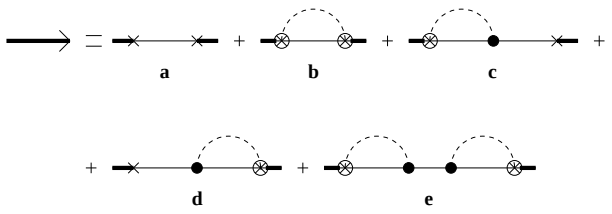

FIG. 4. Dyson equation relating Green's functions G_c (thick solid line) and G_d (thin solid line).

Now we can find the relation between the Green's functions G_c (23) and G_d (5). In leading t approximation it is given by the diagrams presented in figure 4 where the thin solid line represents the bare hole Green's function G_{0d} (7). Each self-energy insertion should be understood as a combination of spin-wave emission and spin-wave absorption diagrams, similar to that in figure 1. Now let us dress these diagrams by higher orders in the hopping t. As we already discussed above, there is no single loop correction to the "dot". We neglect double loop corrections to the "dot" as it has been done in SCBA. Therefore the only possibility is an introduction of self energy corrections to G_d. To take into account all these corrections we need just to replace all bare hole Green's functions G_{0d} by dressed hole Green's functions G_d. So, 4 actually represents a Dyson equation relating G_c (23) and G_d (5). In analytical form it is

$$G_c(\epsilon,\mathbf{k}) = a_{\mathbf{k}}^2 G_d(\epsilon,\mathbf{k}) + \Sigma_1(\epsilon,\mathbf{k}) + 2a_{\mathbf{k}} G_d(\epsilon,\mathbf{k})\Sigma_2(\epsilon,\mathbf{k}) + G_d(\epsilon,\mathbf{k})\Sigma_2^2(\epsilon,\mathbf{k}), \quad (27)$$

where

$$\Sigma_1(\epsilon,\mathbf{k}) = \sum_{\mathbf{q}} [(1+n_{\mathbf{q}}) b_{\mathbf{k-q},\mathbf{q}}^2 G_d(\epsilon-\omega_{\mathbf{q}}, \mathbf{k}-\mathbf{q}) + n_{\mathbf{q}} c_{\mathbf{k},\mathbf{q}}^2 G_d(\epsilon+\omega_{\mathbf{q}}, \mathbf{k}+\mathbf{q})], \qquad (28)$$

and

$$\Sigma_2(\epsilon,\mathbf{k}) = \sum_{\mathbf{q}} [(1+n_{\mathbf{q}}) b_{\mathbf{k-q},\mathbf{q}} g_{\mathbf{k-q},\mathbf{q}} G_d(\epsilon-\omega_{\mathbf{q}}, \mathbf{k}-\mathbf{q}) + n_{\mathbf{q}} c_{\mathbf{k},\mathbf{q}} g_{\mathbf{k},\mathbf{q}} G_d(\epsilon+\omega_{\mathbf{q}}, \mathbf{k}+\mathbf{q})]. \qquad (29)$$

B. Sum rules

Let us check now the sum rules. All singularities of the retarded Green's functions are in the lower half plane of complex ϵ. Therefore if we integrate eq.(19) over ϵ from $-\infty$ to $+\infty$, this integral can be replaced by the integral over an infinite semi-circle in the upper ϵ half plane. For infinite ϵ, $G_d = G_{0d}$, and we get the well known sum rule

$$-\frac{1}{\pi} Im \int_{-\infty}^{\infty} G_d(\epsilon,\mathbf{k}) d\epsilon = 1, \qquad (30)$$

which agrees with eq.(4). If we integrate eq.(27) in the same limits, the terms which contain more than one

Green's function give no contribution, because the integral can be transferred into the upper complex ϵ half plane, and we find

$$-\frac{1}{\pi} Im \int_{-\infty}^{\infty} G_c(\epsilon, \mathbf{k}) d\epsilon = \left(-\frac{1}{\pi} Im \int G_d(\epsilon, \mathbf{k}) d\epsilon \right) \left(a_{\mathbf{k}}^2 + \sum_{\mathbf{q}} \left[(1+n_{\mathbf{q}}) b_{\mathbf{k}-\mathbf{q},\mathbf{q}}^2 + n_{\mathbf{q}} c_{\mathbf{k},\mathbf{q}}^2 \right] \right)$$
$$= 0.5 + \frac{2}{N} \sum_{\mathbf{q}} \left[(1+n_{\mathbf{q}}) v_{\mathbf{q}}^2 + n_{\mathbf{q}} u_{\mathbf{q}}^2 \right]$$
$$= \frac{2}{N} \sum_{\mathbf{q}} \frac{A}{\omega_{\nu \mathbf{q}}} (1+2n_{\mathbf{q}}) = 1, \tag{31}$$

where we have used eqs. (13) and (15). Thus equation (27) reproduces the correct normalization: $\langle 0 | c_{\mathbf{k}\uparrow}^{\dagger} c_{\mathbf{k}\uparrow} | 0 \rangle = 1$. This also proves that the vertices (25) and (26) are correct.

The vertices $b_{\mathbf{k},\mathbf{q}}$ (25) and $c_{\mathbf{k},\mathbf{q}}$ (26) are invariant under translation by the inverse vector of magnetic sublattice $\mathbf{Q} = (\pm\pi, \pm\pi)$: $b_{\mathbf{k}+\mathbf{Q},\mathbf{q}} = b_{\mathbf{k},\mathbf{q}}$. At the same time the vertex $g_{\mathbf{k},\mathbf{q}}$ (17) changes sign with this translation: $g_{\mathbf{k}+\mathbf{Q},\mathbf{q}} = -g_{\mathbf{k},\mathbf{q}}$. Therefore the self energy $\Sigma_2(\epsilon, \mathbf{k})$ changes sign at $\mathbf{k} \to \mathbf{k} + \mathbf{Q}$ and

$$G_c(\epsilon, \mathbf{k}+\mathbf{Q}) \neq G_c(\epsilon, \mathbf{k}). \tag{32}$$

The imaginary part of $G_c(\epsilon, \mathbf{k})$ gives directly the spectra measured in ARPES experiments. This Green's function can be calculated using the Dyson equation (27) as soon as we have found G_d in SCBA (19).

C. Results for $\mathbf{G}_c$

Numerical evaluation of G_c at finite temperature, however, is more complicated than at T=0. The problem lies in the infrared divergence of the integrand of $\Sigma_1(\epsilon, \mathbf{k})$ at small $\mathbf{q}$. To clarify this we compare the small q behavior of the integrands of the self-energies Σ, Σ_1, and Σ_2. Small q means that $1/\xi_M \ll q \ll T$, where $\xi_M \propto \exp(1.1/T)$ is the magnetic correlation length. In this region the spin-wave mean occupation number is $n_{\mathbf{q}} \sim T/q$, and the vertices are $g_{\mathbf{k},\mathbf{q}} \sim \sqrt{q}$, $b_{\mathbf{k},\mathbf{q}} \approx c_{\mathbf{k},\mathbf{q}} \sim 1/\sqrt{q}$. The self energy Σ has an integrand $\propto n_{\mathbf{q}} g_{\mathbf{k},\mathbf{q}}^2 d^2q \sim T q dq$. It is convergent at small q and therefore numerical calculation of Σ is straightforward and the finite temperature generalization of SCBA is as simple as zero temperature SCBA. For the integrand of the self-energy Σ_2 on finds $\propto n_{\mathbf{q}} b_{\mathbf{k},\mathbf{q}} g_{\mathbf{k},\mathbf{q}} d^2q \sim T dq$, which is also convergent at small q. The situation is different in self-energy Σ_1: it is logarithmically divergent at small q: $\propto n_{\mathbf{q}} b_{\mathbf{k},\mathbf{q}}^2 d^2q \sim T dq/q$. There is no real divergence, however, because the integral is convergent at $q \sim 1/\xi_M$, but to calculate this integral numerically by "brute force" one needs a grid with $\Delta q \ll 1/\xi_M$. One then needs for example, when T=0.25, a lattice of at least 200×200, and for lower temperatures an even a bigger lattice.

We can avoid this problem by renormalizing Σ_1, so that we can work with a reasonable grid-size. Let us rewrite eq. (28) in the form

$$\Sigma_1(\epsilon, \mathbf{k}) = \Sigma_R(\epsilon, \mathbf{k}) + \Sigma_{RR}(\epsilon, \mathbf{k}), \tag{33}$$

where

$$\Sigma_R(\epsilon, \mathbf{k}) = \sum_{\mathbf{q}} (1+n_{\mathbf{q}}) b_{\mathbf{k}-\mathbf{q},\mathbf{q}}^2 \left[G_d(\epsilon - \omega_{\mathbf{q}}, \mathbf{k}-\mathbf{q}) - G_d(\epsilon, \mathbf{k}) \right] + \sum_{\mathbf{q}} n_{\mathbf{q}} c_{\mathbf{k},\mathbf{q}}^2 \left[G_d(\epsilon + \omega_{\mathbf{q}}, \mathbf{k}+\mathbf{q}) - G_d(\epsilon, \mathbf{k}) \right], \tag{34}$$

and

$$\Sigma_{RR}(\epsilon, \mathbf{k}) = G_d(\epsilon, \mathbf{k}) \sum_{\mathbf{q}} \left[(1+n_{\mathbf{q}}) b_{\mathbf{k}-\mathbf{q},\mathbf{q}}^2 + n_{\mathbf{q}} c_{\mathbf{k},\mathbf{q}}^2 \right]. \tag{35}$$

Numerical calculation of Σ_R does not cause any trouble because it is well convergent at small q. On the other hand Σ_{RR} can be easily calculated analytically using the modified spin-wave theory equations (13) and (15): $\Sigma_{RR}(\epsilon, \mathbf{k}) = \frac{1}{2} G_d(\epsilon, \mathbf{k})$. Using this procedure the calculation can be done at arbitrary small temperature. The results are practically independent of the grid as soon as it is larger than 20×20. The plots of $-\frac{1}{\pi} Im\ G_c(\epsilon, \mathbf{k})$ as a functions of ϵ for $\mathbf{k} = (\pi/2, \pi/2)$, $\mathbf{k} = (\pi/2, 0)$, and $\mathbf{k} = (\pi, 0)$ are presented in figure 5.

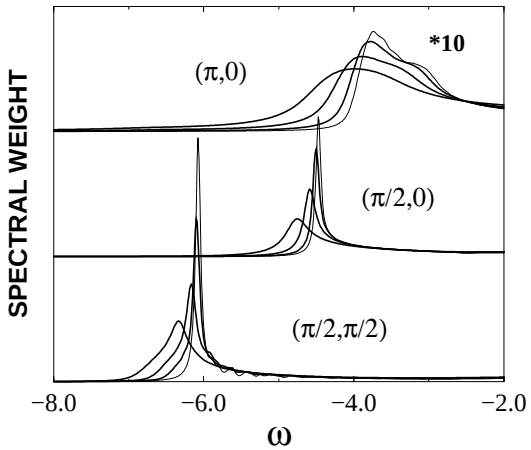

FIG. 5. Plots of $-\frac{1}{\pi} Im\ G_c(\omega, \mathbf{k})$ for different temperatures and $\mathbf{k}$-points. The thin line is the result for $T = 0.01$, the thick lines for $T = 0.2, 0.3$ and 0.4. The spectral weight at the $(\pi, 0)$ point is multiplied by a factor 10.

The half widths of quasiparticle peaks of G_c are slightly larger than the half widths of quasiparticle peaks of G_d. The spectra at T=0.01 quite well agrees with zero temperature calculation[6]. We stress that the agreement is

not trivial. At T=0 long range anti-ferromagnetic order is assumed, and in the present work we used a quite different approach based on a state without long range order. The agreement indicates that these two approaches are consistent. For non-zero temperatures the trend in the spectra for G_c is the same as for G_d; the temperature effect is to shift the quasi-particle peaks uniformly to lower energies and to broaden them. The spectra presented in figure 5 should be directly compared with ARPES experimental data[1,2]. They reasonably reproduce positions and residues of experimental peaks, but fail to reproduce widths of the peaks.

IV. CONCLUSIONS

We considered the two-dimensional $t-t'-t''-J$ model at finite temperature, and developed a technique to deal with the state without long range anti-ferromagnetic order. There is hope to extend this technique to the spin liquid state of the doped system. We generalized the self-consistent Born approximation to the case of nonzero temperature and derived the Dyson equation which relates the single hole Green's function with fixed spin to the single hole Green's function with fixed pseudo-spin. This equation is sensitive to very large distances of order of magnetic correlation length and therefore not convenient for computations. To overcome this problem we developed a renormalization procedure which allows one to exclude large distances and to work with a relatively small lattice: the results are independent of the lattice size as soon as it is larger than 20×20. The effect of a finite temperature is a broadening and a shift of the quasi-particle peaks to lower energy, independent of the momentum. This is attributed to the frustrated magnetic order at finite temperature. The calculated ARPES spectra demonstrate that temperature broadening is not enough to explain widths of the experimental spectra[1,2]. This strengthens the argument that other degrees of freedom contribute to the peak width[6].

V. ACKNOWLEDGMENTS

We are very grateful to M. Kuchiev and G.A. Sawatzky for stimulating discussions. This work was financially supported by the Nederlandse Stichting voor Fundamenteel Onderzoek der Materie (FOM) and the Stichting Scheikundig Onderzoek Nederland (SON), both financially supported by the Nederlandse Organisatie voor Wetenschappelijk Onderzoek (NWO).

[a] Materials Science Center, University of Groningen, Nijenborgh 4, 9747 AG Groningen, The Netherlands.
[b] Also at the Budker Institute of Nuclear Physics, 630090 Novosibirsk, Russia

[1] B. O. Wells *et al*, Phys. Rev. Lett. **74**, 964 (1995).
[2] J. J. Pothuizen *et al*, Phys. Rev. Lett. **78**, 717 (1997).
[3] A. Nazarenko, K. J. E. Vos, S. Haas, E. Dagotto, and R. J. Gooding, Phys. Rev. B **51**, 8676 (1995).
[4] J. Bala, A. M. Oles, and J. Zaanen, Phys. Rev. B **52** 4597 (1995).
[5] O. K. Andersen *et al*, J. Phys. Chem. Solids **56** 1573 (1995).
[6] O. P. Sushkov, G. Sawatzky, R. Eder, and H. Eskes, submitted to Phys. Rev. B.
[7] M. Takahashi Phys. Rev. B **40**, 2494 (1989).
[8] Y. Tokura *et al*, Phys. Rev. B **41**, 11657 (1990).
[9] M. Greven *et al*, Phys. Rev. Lett. **72** 1096 (1994).
[10] S. Schmitt-Rink, C. M. Varma, and A. E. Ruckenstein, Phys. Rev. Lett. **60**, 2793 (1988).
[11] C. L. Kane, P. A. Lee, and N. Read, Phys. Rev. B **39**, 6880 (1989).
[12] G. Martinez and P. Horsch, Phys. Rev. B **44**, 317 (1991).
[13] Z. Liu and E. Manousakis, Phys. Rev. B **45**, 2425 (1992).
[14] O. P. Sushkov, Phys. Rev. B **49**, 1250 (1994).
[15] E. Manousakis, Rev. Mod. Phys. **63**, 1 (1991).
[16] F. J. Dyson, Phys. Rev. **102**, 1217,1230 (1956); S. V. Maleev, Zh. Eksp. Teor. Fiz. **30**, 1010 (1957) [Sov. Phys. JETP **6**, 776 (1958).
[17] R. Eder, Y. Ohta, and G. Sawatzky, Phys. Rev. B **55**, R3414 (1997).